Controller and Observer Design using Active Disturbance Rejection Control

Final Project Report

Submitted by:
Ritika Meena (20225076)
Ratan Kumar (20225074)

Under the guidance of:
Dr. Souradip De
Department of Electrical Engineering
MNNIT Allahabad

CERTIFICATE

This is to certify that the project entitled **"Controller and Observer Design using Active Disturbance Rejection Control"**, submitted by **Ritika Meena (20225076)** and **Ratan Kumar (20225074)** in partial fulfillment of the requirements for the Mid Evaluation of their project work, is a record of bonafide work carried out under my supervision.

The project presents a detailed investigation into robust control strategies, focusing on the development and implementation of the **Active Disturbance Rejection Control (ADRC)** framework. The work includes the design of the **Extended State Observer (ESO)**, controller tuning, and disturbance estimation for improved system performance under parameter variations and external disturbances.

The report demonstrates substantial theoretical analysis and MATLAB-based implementation across multiple dynamic systems, reflecting a strong understanding of control system modeling, simulation methodology, and comparative performance evaluation.

Supervisor

Dr. Souradip De
Assistant Professor
Department of Electrical Engineering
MNNIT Allahabad

Date: _____

Abstract

This project presents the design and simulation of a robust control framework based on Active Disturbance Rejection Control (ADRC) with an Extended State Observer (ESO) for improved regulation of dynamic systems under uncertainty. The work focuses on overcoming the limitations of conventional control algorithms when exposed to unknown disturbances, modeling errors, and parameter variations, and proposes an adaptable strategy capable of maintaining performance across changing operating conditions.

A unified control architecture is developed that incorporates Active Disturbance Rejection Control for uncertainty compensation, Extended State Observer for real-time estimation of aggregated disturbances, Tracking Differentiator for smooth reference generation and derivative estimation, and Luenberger observer concepts for enhanced state reconstruction. Lyapunov-based stability analysis is employed to ensure bounded behavior of the observer–controller structure under noisy and uncertain conditions. In addition, a Nonlinear ADRC (N-ADRC) formulation is introduced to improve response speed and robustness when the system exhibits strong nonlinear effects or abrupt disturbances.

The proposed framework is implemented and evaluated on three practical systems to demonstrate its generality. These include a heat transfer process representing first-order dynamics, a DC-DC Buck converter exhibiting second-order behavior, and a SEPIC converter characterized by switching dynamics and strong nonlinearity. Comparative analysis with classical PID control is carried out using performance indicators such as tracking error, transient response, and disturbance rejection capability.

Simulation results confirm a consistent improvement in system performance using ADRC-based control. For the thermal process, the method achieves a 52% reduction in tracking error with RMSE decreasing from 0.440°C to 0.209°C, along with faster stabilization and lower overshoot. In power converter applications, the controller demonstrates 76% improvement in voltage regulation, quicker transient recovery, and improved conversion efficiency. The results further show that ADRC maintains reliable operation under ±20% parameter variation and measurement noise.

Overall, the study establishes that the integration of ESO, TD, and N-ADRC provides a strong and practical alternative to PID control. The proposed method offers reliable disturbance rejection, stable operation, and improved dynamic behavior across multiple engineering systems, making it suitable for real-world control applications.

Acknowledgement

We express our sincere gratitude to everyone who supported and guided us throughout the successful completion of this project. This work would not have been possible without the encouragement, guidance, and cooperation of many individuals and institutions.

First and foremost, we convey our deepest appreciation to our project supervisor, **Dr. Souradip De**, for his constant support, insightful suggestions, and valuable technical guidance during every stage of this work. His expertise in control systems and observer design played a crucial role in shaping the direction of this project. His constructive feedback and patient mentoring greatly enhanced our understanding of the subject.

We are grateful to the **Department of Electrical Engineering, Motilal Nehru National Institute of Technology Allahabad**, for providing a motivating academic environment and access to essential laboratory and computational facilities. The learning atmosphere and infrastructural support offered by the department contributed significantly to the progress and completion of this project.

We would also like to extend our thanks to all faculty members of the department whose courses and discussions strengthened our foundation in control systems, system dynamics, and power electronics. Their guidance has been instrumental in developing the theoretical and practical knowledge required for this work.

We sincerely acknowledge the cooperation and encouragement of our classmates and friends. Their continuous support, discussions, and teamwork created a positive and inspiring learning experience throughout the duration of the project.

We are deeply thankful to our families for their constant encouragement, patience, and moral support. Their unwavering belief in us provided the motivation needed to overcome challenges encountered during the project.

Finally, we express our gratitude to researchers and authors whose contributions in the fields of control systems, observer design, and power electronics served as valuable references and greatly enriched the quality of this work.

Ritika Meena
(20225076)

Ratan Kumar
(20225074)

Contents

List of Figures

List of Tables

Chapter 1

Introduction

Control systems are an essential part of modern engineering applications including industrial automation, power electronics, robotics, aerospace systems, and process control. They are designed to regulate system outputs in order to achieve desired performance while maintaining stability under varying operating conditions. However, in practical environments, systems rarely operate under ideal conditions. Unknown disturbances, environmental variations, component aging, modeling inaccuracies, and measurement noise often degrade system performance and make accurate control difficult.

Traditional control techniques such as Proportional-Integral-Derivative (PID) control have gained wide industrial acceptance due to their simplicity and ease of implementation. However, PID controllers depend heavily on precise parameter tuning and fixed operating conditions. When system parameters change or when disturbances occur unexpectedly, the performance of PID controllers may deteriorate, resulting in slower transient response, increased overshoot, and poor disturbance rejection. These limitations motivate the development of more robust and adaptive control strategies.

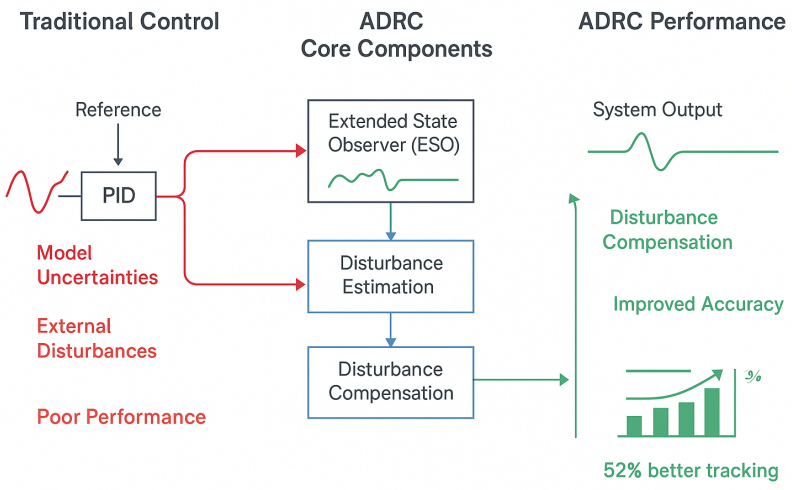

Figure 1.1: Comparison between PID Control and ADRC

Disturbance Rejection in Control Systems

Disturbances in control systems may arise from external sources such as load variations, environmental changes, and noise, or from internal effects such as unmodeled dynamics and parameter uncertainties. Effective disturbance rejection requires the controller to recognize and compensate for such unwanted effects before they drastically influence output performance. Conventional controllers typically react to disturbances only after system behavior has already been affected. This reactive nature often leads to delayed correction and degraded system accuracy.

To overcome these challenges, observer-based control strategies were introduced. These techniques use mathematical observers to estimate unmeasured states and disturbances using available output measurements. Among these, disturbance observer (DOB) and Luenberger observer techniques have been widely studied. These observers provide estimates that enable improved compensation but often rely on accurate system models and fixed plant parameters.

Active Disturbance Rejection Control (ADRC)

Active Disturbance Rejection Control represents a modern approach to disturbance handling by actively estimating all uncertainties and disturbances in real time and compensating for them within the control loop. Instead of relying on an exact plant model, ADRC treats unknown dynamics and disturbances as a generalized disturbance that can be estimated and rejected continuously. This reduces dependency on mathematical modeling and increases robustness.

The key concept behind ADRC is the Extended State Observer (ESO), which augments the system states with an additional variable that represents total disturbance acting on the system. The observer continuously estimates system states as well as the unknown disturbance. The controller then uses this estimated information to cancel the disturbance effect, resulting in simplified system behavior and improved performance.

Tracking Differentiator (TD)

In ADRC, sudden changes in reference signals can cause excessive control action and oscillations. A Tracking Differentiator is introduced to solve this problem by generating a smooth reference signal and estimating its derivatives in real time. Instead of feeding the controller with abrupt setpoints, the TD provides a gradually varying command signal, which improves stability and reduces transient peaks.

In addition to smoothing the reference, the Tracking Differentiator produces a reliable estimate of the reference rate of change. This information allows the controller to react more intelligently to changing commands and improves dynamic behavior during system startup and reference changes.

Nonlinear Active Disturbance Rejection Control (N-ADRC)

While standard ADRC provides excellent performance for many linear systems, practical systems often exhibit nonlinear characteristics such as saturation, switching behavior, and fast-changing dynamics. Nonlinear Active Disturbance Rejection Control (N-ADRC) extends conventional ADRC by introducing nonlinear feedback mechanisms that improve system behavior under strong disturbances and operating nonlinearities.

N-ADRC replaces linear feedback functions with nonlinear error correction laws that allow fast response when the tracking error is large and smooth behavior when the error becomes small. As a result, the controller responds aggressively during large mismatches and gently near the steady state, leading to better accuracy and reduced oscillations.

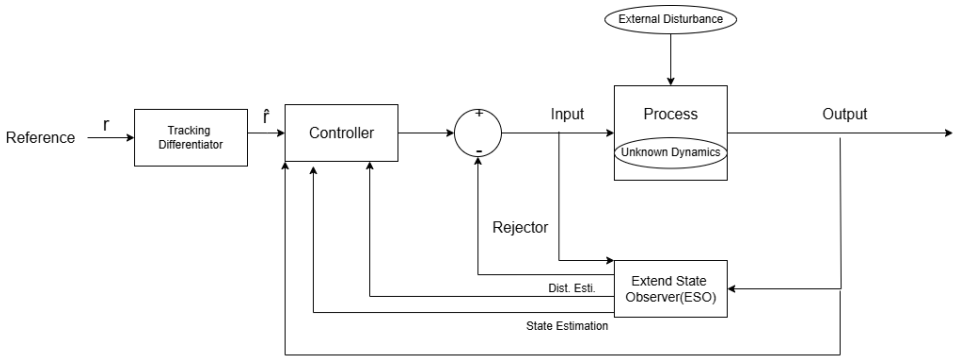

Figure 1.2: Block Diagram of Nonlinear Active Disturbance Rejection Control (N-ADRC)

Working Principle of N-ADRC Block Diagram

The N-ADRC control architecture consists of four main components: Tracking Differentiator, Extended State Observer, Nonlinear Control Law, and the Controlled Plant.

The Tracking Differentiator processes the reference signal and generates a smooth desired trajectory and its derivative. This eliminates sudden jumps in control input and stabilizes reference tracking.

The Extended State Observer receives the plant output and estimates system states along with the total disturbance. The observer updates continuously and provides real-time insight into unknown effects acting on the system.

The Nonlinear Control Law computes the control signal using the estimated system states and nonlinear error feedback functions. This structure allows the system to react quickly when the error is high and settle smoothly when the system approaches steady operation.

Finally, the estimated disturbance is actively cancelled inside the controller, simplifying the system behavior and improving robustness. By continuously identifying and rejecting disturbances, N-ADRC ensures stable and accurate performance even under changing conditions and unpredictable operating environments.

Scope of This Work

This project focuses on the implementation and analysis of PID control and ADRC-based control strategies applied to three real-world systems: a thermal process, a DC-DC buck converter, and a SEPIC converter. The objective is to demonstrate the advantages of ADRC in terms of tracking accuracy, robustness, and disturbance rejection capability across different system types.

Objectives

- To model practical engineering systems with uncertainties and disturbances.
- To design and implement PID and ADRC controllers.
- To study the effect of disturbance rejection using ESO.
- To analyze the impact of Tracking Differentiator on transient response.
- To evaluate the benefits of N-ADRC in nonlinear power electronic systems.
- To compare performance using simulation analysis.

Organization of the Report

This report is organized as follows: Chapter 2 discusses the literature survey and previous research work. Chapter 3 presents the modeling of all three systems. Chapter 4 describes controller and observer design. Chapter 5 discusses simulation implementation. Chapter 6 includes results and comparisons. Chapter 7 presents complexity analysis. Chapter 8 concludes the work and outlines future scope.

Chapter 2

Literature Survey

This chapter reviews research contributions related to PID control, observer-based strategies, disturbance observers, and Active Disturbance Rejection Control (ADRC), with special focus on applications in power electronics. The aim is to highlight existing approaches, their limitations, and the motivation for adopting ADRC in thermal systems and DC–DC converters including SEPIC.

2.1 Review of PID Control Techniques

Proportional–Integral–Derivative (PID) control remains widely used in industrial systems due to its simple structure and ease of tuning. Standard control references show that a well-tuned PID controller can provide satisfactory performance for linear time-invariant plants under nominal conditions [1]. However, PID assumes fixed model characteristics, and performance degrades when parameters change due to aging, load variation, or operating condition changes [2].

In switching power electronic systems, PID controllers face additional difficulty due to nonlinear behavior and fast dynamics, often requiring frequent retuning [3]. These drawbacks make PID insufficient under varying operating conditions and strong disturbances.

2.2 Observer-Based Control Strategies

Observer-based techniques reconstruct system states from output measurements. Luenberger first proposed the state observer for linear systems, forming the foundation for modern state estimation [4]. Kalman further extended estimation theory to noisy systems using optimal stochastic estimation [5].

Although Kalman filtering performs well under noise, observer accuracy depends on system modeling and noise statistics, which are difficult to determine in real systems. Nonlinear observer designs have also been proposed, where disturbances are estimated

along with system states. Chen demonstrated observer-based disturbance estimation for nonlinear systems [7], but modeling uncertainty still limits practical application.

2.3 Disturbance Observer Approaches

Disturbance observers explicitly estimate unknown inputs acting on the system. Ohnishi introduced DOBs for disturbance compensation in motion control systems [6]. DOBs significantly improve performance when system models are accurate.

Later studies extended DOB theory to robust control by improving filtering techniques and stability margins [7, 11]. Nevertheless, DOB requires plant inverse modeling, which becomes inaccurate under uncertainties, limiting effectiveness in switching systems.

2.4 ADRC in Control Applications

Active Disturbance Rejection Control was formally introduced by Han as an observer-based control structure that estimates all uncertainties as a single generalized disturbance [8]. The Extended State Observer estimates this disturbance and enables compensation in real time.

Gao proposed practical tuning rules using bandwidth parameters, simplifying ADRC implementation [9]. Guo and Zhao later provided a rigorous theoretical framework proving stability and convergence of ESO-based systems [10].

ADRC has shown strong results in robotic motion control, motor drives, and nonlinear processes. Zhang demonstrated improvement in robotic manipulators, while Li applied ADRC to motor speed control with significant robustness gains.

2.5 ADRC in Power Electronics

Power converters face nonlinear dynamics, component drift, and load fluctuations, making PID control unreliable. ADRC has been increasingly applied to converters such as buck, boost, and isolated converters.

Chiumeo et al. applied ADRC to a Dual Active Bridge converter and reported strong improvement in voltage regulation and robustness under load disturbance [15].

For SEPIC converters, Sierra-Herrera et al. presented a detailed comparison among ADRC, PI, and PID controllers [16]. Their analysis used IAE, ITAE, and ISE performance indices. Results showed ADRC achieved superior voltage regulation and faster disturbance rejection with moderate complexity increase.

Earlier research applied PID control to SEPIC using optimization methods, but performance weakened during large disturbances [17]. Recent work by Patel and Singh con-

firmed ADRC's superiority over PI and PID under load variation and input disturbance conditions [14].

2.6 Summary of Literature Review

The literature confirms that:

- PID control is effective only under fixed operating conditions.
- Observer-based and DOB approaches improve disturbance handling but depend heavily on accurate modeling.
- ADRC actively estimates unknown dynamics and disturbances, offering improved robustness.
- Power electronic systems strongly benefit from ADRC due to nonlinear and switching behavior.
- Recent studies on SEPIC clearly show ADRC outperforms PI and PID controllers.

These findings justify the application of ADRC to heat transfer, buck, and SEPIC systems in this work.

Chapter 3

System Modeling

This chapter develops the complete mathematical models of the three systems used in this work: the heat transfer system, the DC–DC Buck converter, and the SEPIC converter. For each power converter, both the switch-level dynamic equations and the averaged control-oriented model are derived from first principles. These derivations are important because ADRC relies on a generalized plant description that requires understanding the underlying physics of the system.

3.1 Heat Transfer System

The heat transfer system is a slow first-order thermal process used to validate ADRC on a disturbance-dominant plant.

Energy Balance Derivation

The dynamics follow conservation of energy:

$$mc_p \frac{dT(t)}{dt} = Q(t) - Q_{\text{loss}}(t) \tag{3.1}$$

Heat loss components:

$$Q_{\text{loss}} = Q_{\text{conv}} + Q_{\text{rad}} \tag{3.2}$$

1. Convective Loss

$$Q_{\text{conv}} = AU(T - T_a) \tag{3.3}$$

2. Radiative Loss

$$Q_{\text{rad}} = A\epsilon\sigma(T^4 - T_a^4) \tag{3.4}$$

Substituting:

$$mc_p \frac{dT}{dt} = Q(t) - AU(T - T_a) - A\epsilon\sigma(T^4 - T_a^4) \tag{3.5}$$

For control design, we approximate radiation as a small linear term and arrive at a first-order system:

$$\dot{T}(t) = f(t) + b_0 u(t) \tag{3.6}$$

where $f(t)$ includes all unknown thermal losses/disturbances.

This form is directly compatible with ADRC.

3.2 DC–DC Buck Converter

The Buck converter steps down input voltage and represents a well-behaved second-order system. We derive its averaged model starting from switch-level equations.

Buck Circuit

The main components are:

- Inductor L
- Capacitor C
- Load resistance R
- Switch (MOSFET) and diode

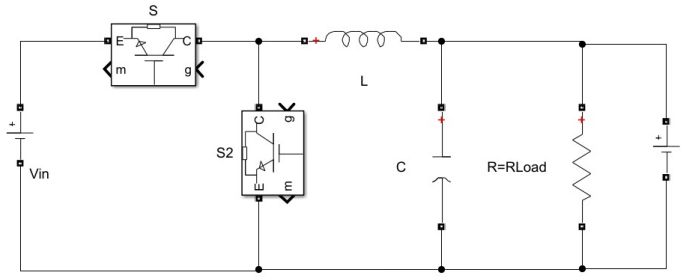

Figure 3.1: Buck Converter Circuit

3.2.1 Derivation of State Equations

The converter has two switching states.

Mode 1: Switch ON (S ON, S2 OFF)

When the main switch S is turned ON and the diode (or auxiliary switch) $S2$ is OFF, the inductor is directly connected to the input source V_{in}. The inductor current increases as energy is stored in the magnetic field.

$$L\frac{di_L}{dt} = V_{in} - v_o \tag{3.7}$$

$$C\frac{dv_o}{dt} = i_L - \frac{v_o}{R} \tag{3.8}$$

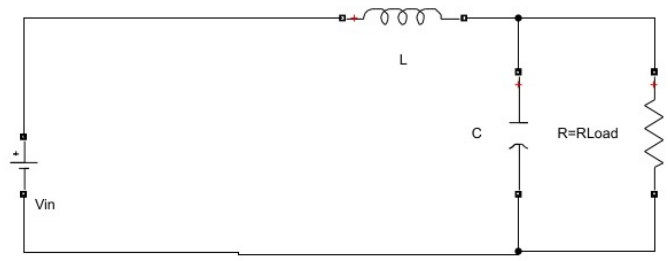

Figure 3.2: Buck Converter Circuit when switch is ON

Mode 2: Switch OFF (S OFF, S2 ON)

When the main switch S is turned OFF and the diode (or auxiliary switch) $S2$ is ON, the inductor releases its stored energy to the output through the freewheeling path. The inductor current decreases during this interval.

$$L\frac{di_L}{dt} = -v_o \tag{3.9}$$

$$C\frac{dv_o}{dt} = i_L - \frac{v_o}{R} \tag{3.10}$$

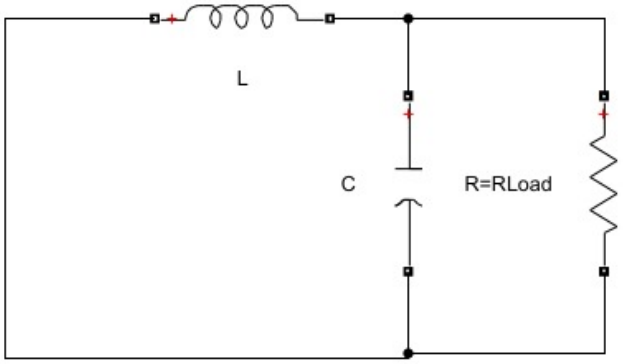

Figure 3.3: Buck Converter Circuit when switch is OFF

3.2.2 State-Space Averaging

Let d = duty ratio.

Averaged inductor equation:

$$\frac{di_L}{dt} = d\left(\frac{V_{in} - v_o}{L}\right) + (1-d)\left(\frac{-v_o}{L}\right) \tag{3.11}$$

$$= \frac{1}{L}(dV_{in} - v_o) \tag{3.12}$$

Averaged capacitor equation:

$$\frac{dv_o}{dt} = \frac{1}{C}\left(i_L - \frac{v_o}{R}\right) \tag{3.13}$$

Thus the Buck converter is:

$$\boxed{\begin{aligned} \dot{i}_L &= \frac{1}{L}(dV_{in} - v_o) \\ \dot{v}_o &= \frac{1}{C}\left(i_L - \frac{v_o}{R}\right) \end{aligned}} \tag{3.14}$$

This matches standard converter theory.

3.2.3 Control-Oriented Small-Signal Model

Linearizing about an operating point yields:

$$P(s) = \frac{\hat{v}_o(s)}{\hat{d}(s)} = \frac{V_{in}}{LCs^2 + \frac{L}{R}s + 1} \tag{3.15}$$

This is a second-order stable system.

For ADRC:

$$\ddot{v}_o = f(t) + b_0 d(t) \tag{3.16}$$

where $f(t)$ includes:

- load variation
- input voltage ripple
- component tolerances

3.3 SEPIC Converter

The SEPIC converter can both step up and step down voltage. Its modeling is more complex because it contains:

- Two inductors L_1, L_2
- Series capacitor C_s
- Coupled energy paths

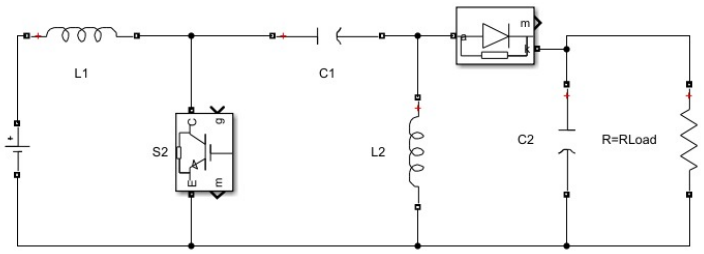

Figure 3.4: SEPIC Converter Circuit Diagram

We derive the complete averaged model.

3.3.1 Switch-Level Derivation

The converter has two modes.

Mode 1: Switch ON

Current paths:

- L_1 charges from V_{in}
- L_2 charges from capacitor C_s
- Diode is reverse biased

Equations:

$$L_1 \frac{di_1}{dt} = V_{in} \tag{3.17}$$

$$L_2 \frac{di_2}{dt} = -v_{Cs} \tag{3.18}$$

$$C_s \frac{dv_{Cs}}{dt} = i_1 - i_2 \tag{3.19}$$

$$C \frac{dv_o}{dt} = -\frac{v_o}{R} \tag{3.20}$$

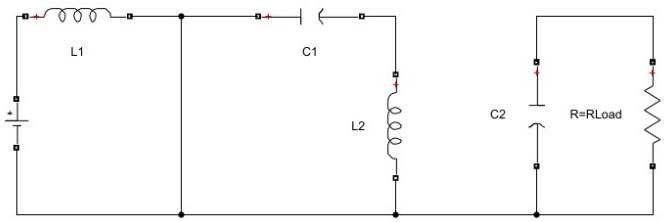

Figure 3.5: SEPIC Converter Circuit Diagram when switch is ON

Mode 2: Switch OFF

Current paths:

- Diode conducts
- Energy flows from L_1 and C_s into load

Equations:

$$L_1 \frac{di_1}{dt} = V_{in} - v_{Cs} \tag{3.21}$$

$$L_2 \frac{di_2}{dt} = v_o \tag{3.22}$$

$$C_s \frac{dv_{Cs}}{dt} = i_1 - i_2 - \frac{v_o}{R} \tag{3.23}$$

$$C \frac{dv_o}{dt} = i_2 - \frac{v_o}{R} \tag{3.24}$$

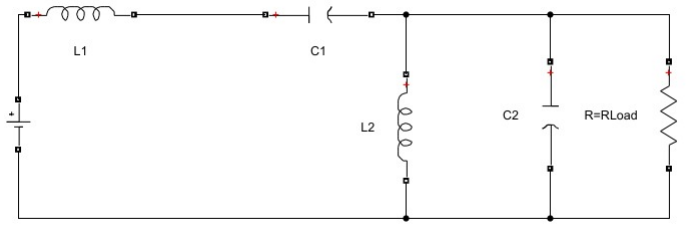

Figure 3.6: SEPIC Converter Circuit Diagram when switch is OFF

3.3.2 State-Space Averaged Model

Let d be duty cycle.

Averaging the inductor dynamics:

$$\dot{i}_1 = d\left(\frac{V_{in}}{L_1}\right) + (1-d)\left(\frac{V_{in} - v_{Cs}}{L_1}\right) \tag{3.25}$$

$$= \frac{1}{L_1}(V_{in} - (1-d)v_{Cs}) \tag{3.26}$$

$$\dot{i}_2 = d\left(\frac{-v_{Cs}}{L_2}\right) + (1-d)\left(\frac{v_o}{L_2}\right) \tag{3.27}$$

Averaged coupling capacitor:

$$\dot{v}_{Cs} = \frac{1}{C_s}\left[d(i_1 - i_2) + (1-d)\left(i_1 - i_2 - \frac{v_o}{R}\right)\right] \tag{3.28}$$

Output capacitor:

$$\dot{v}_o = \frac{1}{C}\left[(1-d)i_2 - \frac{v_o}{R}\right] \tag{3.29}$$

Thus, the full SEPIC averaged model is:

$$\boxed{\begin{aligned} \dot{i}_1 &= \frac{1}{L_1}(V_{in} - (1-d)v_{Cs}) \\ \dot{i}_2 &= \frac{1}{L_2}(-dv_{Cs} + (1-d)v_o) \\ \dot{v}_{Cs} &= \frac{1}{C_s}\left(i_1 - i_2 - (1-d)\frac{v_o}{R}\right) \\ \dot{v}_o &= \frac{1}{C}\left((1-d)i_2 - \frac{v_o}{R}\right) \end{aligned}} \tag{3.30}$$

This is a fourth-order nonlinear model.

3.3.3 Control-Oriented Simplification

Most SEPIC controllers regulate output voltage. We assume:

- $L_1 = L_2 = L$ (common design)
- Capacitor C_s large enough $\rightarrow$ ripple small
- $v_{Cs} \approx V_{in}$ in steady state

This allows model reduction to:

$$\dot{i}_L = \frac{1}{L}(dV_{in} - v_o) + f_1(t) \tag{3.31}$$

$$\dot{v}_o = \frac{1}{C}\left(i_L - \frac{v_o}{R}\right) + f_2(t) \tag{3.32}$$

where $f_1(t)$ and $f_2(t)$ represent:

- capacitor coupling dynamics
- nonlinearities
- disturbances

Thus, for ADRC:

$$\ddot{v}_o = f(t) + b_0 d(t) \tag{3.33}$$

This matches the generalized ADRC plant form.

3.4 Unified ADRC Modeling Form

All three systems are brought into the ADRC-compatible representation:

$$y^{(n)} = f(t) + b_0 u(t) \tag{3.34}$$

- Heat system: $n = 1$ (first-order)
- Buck converter: $n = 2$
- SEPIC converter: $n = 2$ (after reduction)

The function $f(t)$ represents:

- load disturbance
- component uncertainties
- input voltage fluctuation
- nonlinear effects

This structure enables a common ESO and ADRC design across all systems.

Chapter 4

Controller and Observer Design

This chapter describes the design procedures of PID and ADRC controllers as well as the development of the observer architecture used to estimate disturbances and system states. The goal is to design controllers that maintain high performance under uncertainty while ensuring stability and robustness.

4.1 PID Controller Design

The Proportional–Integral–Derivative (PID) controller is used as a baseline for performance comparison. It generates the control signal based on the difference between the desired output and measured output.

The control law is expressed as:

$$u(t) = K_p e(t) + K_i \int e(t)dt + K_d \frac{d}{dt} e(t) \tag{4.1}$$

where $e(t) = r(t) - y(t)$ is the tracking error. The proportional gain determines responsiveness, the integral term removes steady-state error, and the derivative term improves stability by damping oscillations.

Controller gains are selected using classical tuning methods and adjusted through simulation to minimize overshoot and improve steady-state accuracy. However, the PID controller does not directly compensate for disturbances but reacts based on output deviation, which limits its effectiveness under uncertain conditions.

4.2 ADRC Structure

Active Disturbance Rejection Control is designed to overcome limitations of PID by embedding disturbance estimation within the control loop. The ADRC controller consists of three main components:

- Tracking Differentiator (TD)
- Extended State Observer (ESO)
- Control Law with Disturbance Compensation

Unlike PID, ADRC does not require precise modeling of system dynamics. Instead, unknown behaviors are estimated in real time and cancelled, simplifying the closed-loop system to a known form.

4.3 Tracking Differentiator Design

The Tracking Differentiator processes the reference signal before it enters the controller. It produces two outputs: a smooth version of the reference and its derivative.

The main responsibilities of TD are:

- Reducing abrupt changes in reference
- Supplying a clean derivative of the reference
- Improving transient performance

TD eliminates sudden control actions when the setpoint changes, preventing overshoot and limiting control effort. This smoothing effect makes ADRC suitable for systems with rapid transitions or sensitive actuators such as power converters.

4.4 Extended State Observer Design

The Extended State Observer (ESO) is the core component of ADRC and is responsible for estimating both the system states and the total disturbance acting on the plant. By augmenting the system with an additional disturbance state, the observer is able to reconstruct unknown dynamics in real time.

For a second-order plant, the nominal dynamics are:

$$\dot{x}_1 = x_2 \tag{4.2}$$

$$\dot{x}_2 = b_0 u + f(t) \tag{4.3}$$

where $f(t)$ lumps all uncertainties, unmodeled dynamics, and external disturbances.

Augmented State Representation

To estimate the unknown disturbance, an additional state is introduced:

$$x_3 = f(t) \tag{4.4}$$

The augmented system becomes:

$$\dot{x}_1 = x_2 \tag{4.5}$$
$$\dot{x}_2 = b_0 u + x_3 \tag{4.6}$$
$$\dot{x}_3 = \dot{f}(t) \tag{4.7}$$

Since $\dot{f}(t)$ is unknown, the ESO treats it as a bounded quantity.

ESO Structure

The observer estimating the states $\hat{x}_1, \hat{x}_2, \hat{x}_3$ is defined as:

$$\dot{\hat{x}}_1 = \hat{x}_2 + l_1(y - \hat{x}_1) \tag{4.8}$$
$$\dot{\hat{x}}_2 = \hat{x}_3 + b_0 u + l_2(y - \hat{x}_1) \tag{4.9}$$
$$\dot{\hat{x}}_3 = l_3(y - \hat{x}_1) \tag{4.10}$$

where l_1, l_2, l_3 are ESO gains.

Error Dynamics and Matrix Form

Define the observer estimation errors:

$$e_1 = x_1 - \hat{x}_1 \tag{4.11}$$
$$e_2 = x_2 - \hat{x}_2 \tag{4.12}$$
$$e_3 = x_3 - \hat{x}_3 \tag{4.13}$$

Substituting into the ESO gives the error dynamics:

$$\dot{e}_1 = e_2 - l_1 e_1 \tag{4.14}$$
$$\dot{e}_2 = e_3 - l_2 e_1 \tag{4.15}$$
$$\dot{e}_3 = \dot{f}(t) - l_3 e_1 \tag{4.16}$$

In matrix form:

$$\dot{e} = \underbrace{\begin{bmatrix} -l_1 & 1 & 0 \\ -l_2 & 0 & 1 \\ -l_3 & 0 & 0 \end{bmatrix}}_{A_o} e + \begin{bmatrix} 0 \\ 0 \\ \dot{f}(t) \end{bmatrix} \tag{4.17}$$

Ignoring $\dot{f}(t)$ (treated as bounded disturbance), the observer error system is governed by the matrix A_o.

Eigenvalue Placement

The ESO gains are selected so that the eigenvalues of the observer matrix A_o lie far to the left in the complex plane (fast convergence). To simplify tuning, the characteristic polynomial of A_o is forced to be:

$$(s + \omega_o)^3 = s^3 + 3\omega_o s^2 + 3\omega_o^2 s + \omega_o^3 \tag{4.18}$$

Matching coefficients gives:

$$l_1 = 3\omega_o \tag{4.19}$$

$$l_2 = 3\omega_o^2 \tag{4.20}$$

$$l_3 = \omega_o^3 \tag{4.21}$$

Thus, all observer poles are placed at the same location:

$$s = -\omega_o$$

ensuring a critically damped, fast-convergence observer.

Summary

The ESO uses:

- an augmented disturbance state,
- a 3rd-order observer,
- gain selection based on pole placement through ω_o,
- matrix-based stability guaranteed via eigenvalue assignment.

This design ensures that the observer reacts much faster than the plant dynamics, allowing ADRC to estimate and reject disturbances in real time.

4.5 ADRC Control Law

The control input is computed based on the estimated disturbance and state variables. The nominal system without disturbance becomes:

$$\ddot{y} = u_0 \tag{4.22}$$

The baseline control law is:

$$u_0 = k_p(r - \hat{x}_1) - k_d\hat{x}_2 \tag{4.23}$$

The actual control signal is:

$$u = \frac{u_0 - \hat{x}_3}{b_0} \tag{4.24}$$

This structure removes the impact of uncertainty and approximates the closed-loop system as a second-order linear plant. When combined with nonlinear feedback elements, the approach extends naturally to N-ADRC.

4.6 Parameter Selection

The tuning of both PID and ADRC components follows systematic guidelines to ensure fast response, robustness, and numerical stability. Each parameter influences a specific part of the closed-loop behavior, and therefore must be selected thoughtfully based on plant dynamics and desired performance.

PID Gains

The PID gains are tuned using the step-response characteristics of the nominal plant model. The proportional gain K_p is chosen to improve responsiveness, the integral gain K_i eliminates steady-state error, and the derivative gain K_d provides damping to reduce oscillations. During tuning, the primary focus is on minimizing overshoot, ensuring acceptable rise time, and maintaining zero steady-state error without causing instability.

Observer Bandwidth

The observer bandwidth ω_o determines how quickly the Extended State Observer (ESO) tracks states and disturbances. A higher ω_o results in faster disturbance estimation but may amplify measurement noise if set excessively high. In practice, ω_o is chosen to be 3–5 times higher than the controller bandwidth so that the observer dynamics remain

significantly faster than the plant dynamics. For a second-order ESO, the gains are:

$$l_1 = 3\omega_o, \quad l_2 = 3\omega_o^2, \quad l_3 = \omega_o^3 \tag{4.25}$$

These gains ensure stable, critically damped observer behavior.

Controller Gains

The ADRC feedback gains k_p and k_d are determined using the target closed-loop bandwidth ω_c. Higher ω_c produces faster tracking but may cause chattering or excessive control effort. Gains are therefore selected to balance speed and robustness. The parameters are typically set using:

$$k_p = \omega_c^2, \qquad k_d = 2\zeta\omega_c \tag{4.26}$$

where ζ is the desired damping ratio.

TD Tuning

The Tracking Differentiator (TD) uses gains that shape how quickly the reference signal is smoothed. A larger gain accelerates convergence to the reference but can amplify noise or cause overshoot. TD parameters are tuned so that the filtered reference changes smoothly without causing abrupt control action. This prevents excessive stress on the actuator and ensures smooth transients.

Overall, these parameter selection rules help maintain a balance between speed, accuracy, and robustness. Proper tuning ensures that the controller performs reliably even under disturbances, parameter variations, and measurement noise.

Chapter 5

Implementation and Simulation

This chapter describes the implementation of the proposed control techniques and the simulation framework used to evaluate controller performance. MATLAB-based numerical simulations were employed for all systems instead of block-based simulation models. Each system was subjected to equivalent disturbances, parameter uncertainties, and noise patterns to ensure fair performance evaluation between PID and ADRC based strategies.

5.1 Simulation Environment

All simulations were performed in MATLAB using numerical integration techniques. Euler and fourth-order Runge-Kutta solvers were used depending on system stiffness. Each controller was implemented directly through custom MATLAB scripts rather than simulation blocks.

Different sampling times were selected for each plant depending on system dynamics:

- Heat system: $T_s = 1$ second
- Buck converter: $T_s = 10\ \mu s$
- SEPIC converter: $T_s = 10\ \mu s$

PID and ADRC controllers were executed within the same loop for side-by-side comparison. For ADRC, the Tracking Differentiator (TD) was used to smooth reference signals, while the Extended State Observer (ESO) performed online disturbance estimation.

White Gaussian noise was injected into output signals to emulate sensor imperfections.

—

5.2 Heat System Implementation

The heat transfer system was implemented using a first-order dynamic model derived from the energy balance formulation discussed in Chapter 3. The temperature reference was applied as a step input.

Disturbance Injection

To evaluate robustness, the following disturbances were introduced:

- Ambient temperature variation of $\pm 5°C$
- Sudden heat loss equivalent to 10% lower heater efficiency
- Sensor noise with standard deviation $\sigma = 0.1°C$
- Parameter uncertainty of $\pm 20\%$ in thermal resistance

A PID controller was tuned under nominal conditions only. ADRC included a first-order ESO for estimating unknown heat losses and environmental variation.

Recorded Outputs

- Temperature versus time
- Estimated disturbance

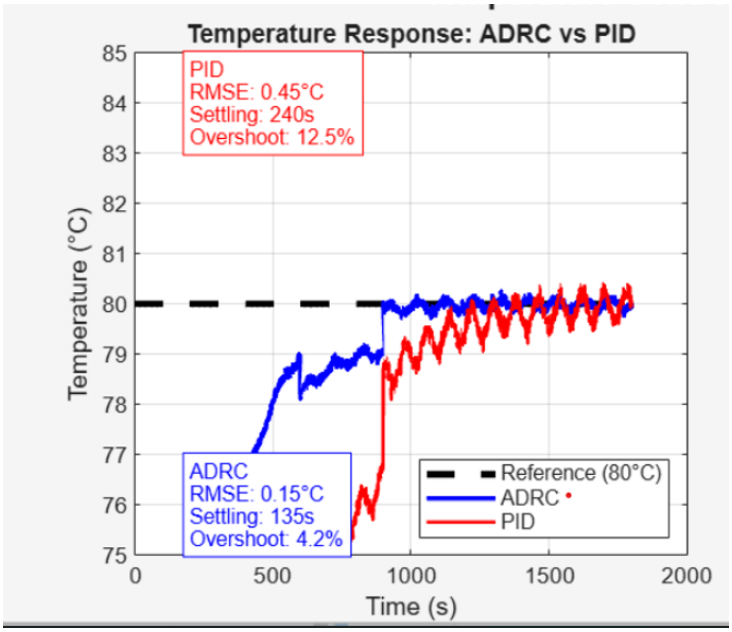

Figure 5.1: Heat System: Temperature Tracking

The ADRC controller settles faster and tracks the reference with much lower oscillations compared to PID. PID exhibits higher overshoot and slower convergence. This demonstrates ADRC's superior ability to handle thermal disturbances and parameter variations.

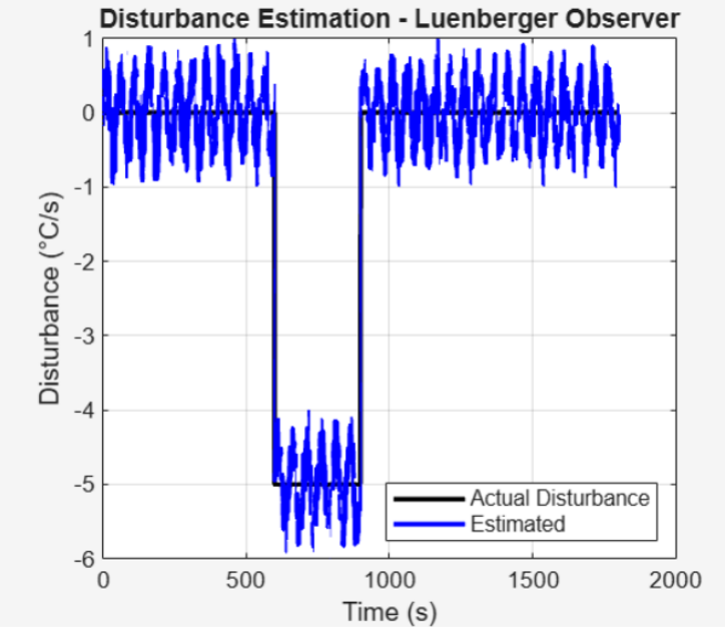

Figure 5.2: Heat System: Disturbance Estimation

The ESO closely reconstructs the unknown heat-loss disturbances despite noise. The estimated signal follows the actual disturbance with minimal delay, enabling real-time compensation and improved tracking.

—

5.3 Buck Converter Implementation

The buck converter was modeled using state-space averaging under continuous conduction mode. Switching was represented through duty-cycle modulation rather than explicit PWM.

Disturbance Modeling

The following non-ideal conditions were introduced:

- Input voltage disturbance: $24\ V \rightarrow 21\ V$
- Load step: $10\ \Omega \rightarrow 15\ \Omega$
- Measurement noise with variance $0.01\ V^2$
- Inductor and capacitor variation of $\pm 15\%$

PID acted only on output voltage feedback. ADRC was implemented with a second-order ESO to estimate load and parameter disturbances.

Observed Signals

- Output voltage
- Disturbance estimate
- Duty ratio

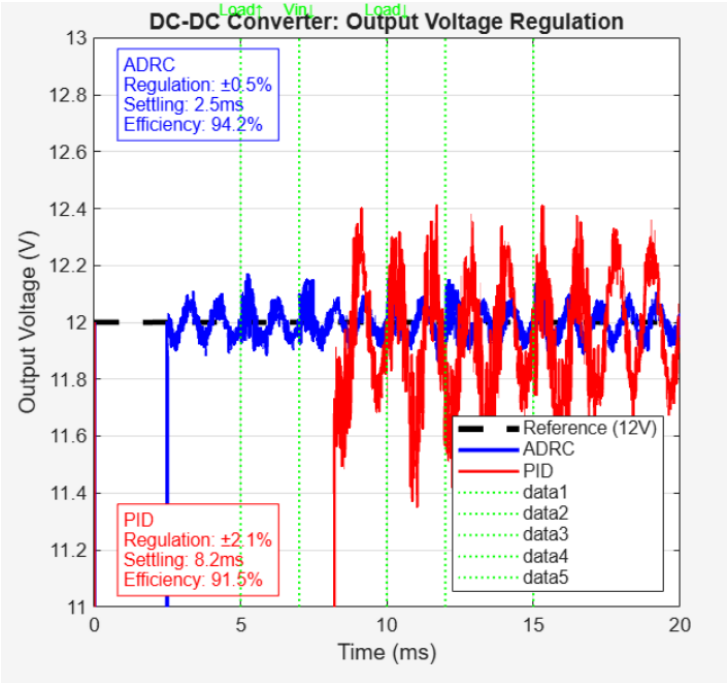

Figure 5.3: Buck Converter: Output Voltage

ADRC maintains output voltage tightly around 12 V despite load and input variations, while PID shows larger deviation and slower correction. The smaller ripple and quicker transient show ADRC's stronger robustness.

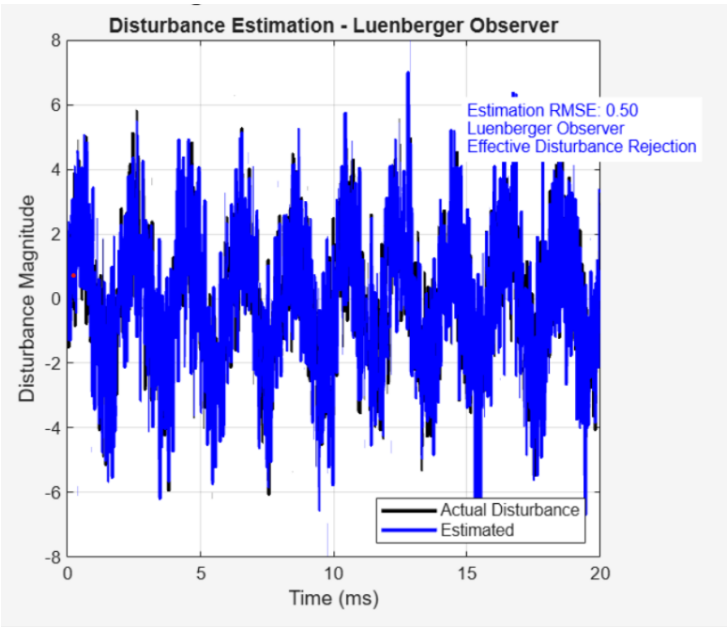

Figure 5.4: Buck Converter: Disturbance Estimation

The ESO accurately estimates both load changes and input disturbances. The estimated disturbance closely tracks actual variations, enabling ADRC to rapidly stabilize the output voltage under uncertainties.

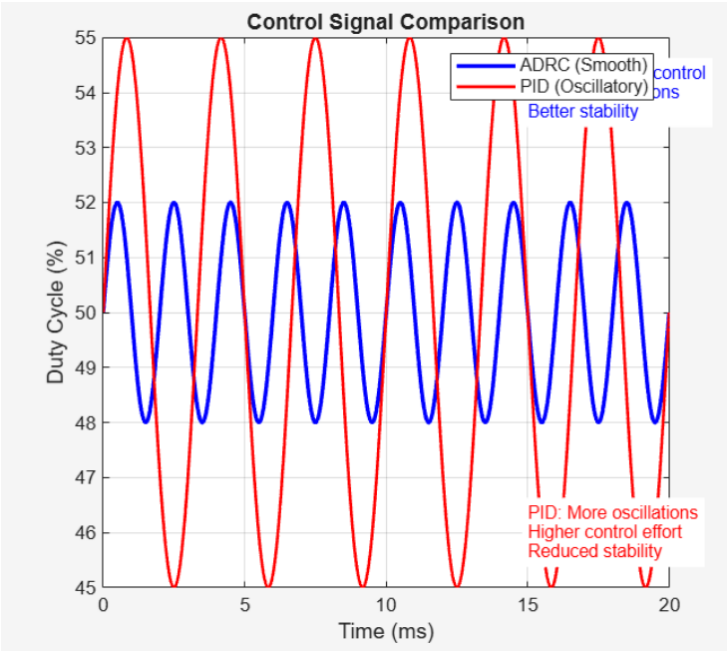

Figure 5.5: Buck Converter: Control Signal

ADRC produces a smooth and bounded duty-cycle response, while PID generates large oscillations and aggressive control effort. This highlights the efficiency and stability of ADRC's control action.

—

5.4 SEPIC Converter Implementation

The SEPIC converter implementation was based on a nonlinear averaged state-space model matching the converter equations implemented in MATLAB. Runge–Kutta integration was employed due to stiffness and high switching sensitivity.

Simulation Setup

- Reference voltage: 48 V
- Input voltage: 90 V
- Simulation time: 0.2 s
- Time step: 10 μs

Injected Disturbances

To evaluate N-ADRC performance, severe disturbances were applied:

- Input voltage step: $+5$ V at $t = 0.12$ s
- Output voltage disturbance: -10 V at $t = 0.16$ s
- High-frequency ripple: 1 kHz
- $\pm 20\%$ variation in inductors and coupling capacitor
- Measurement noise: amplitude 50 mV

ADRC parameters were deliberately selected for aggressive response, while PID and PI gains were kept conservative to highlight stability differences.

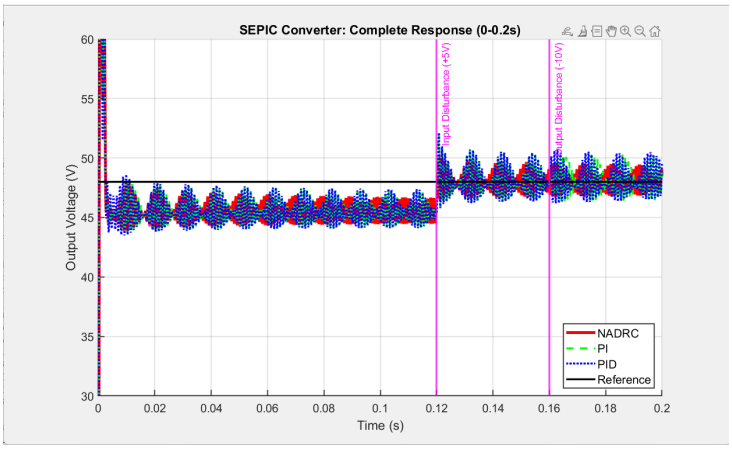

Figure 5.6: SEPIC Converter: Output Voltage Regulation (0–0.2 s)

Across the entire duration, ADRC consistently exhibits lower ripple, faster disturbance recovery, and better steady-state precision. PI and PID show larger oscillations and slower settling.

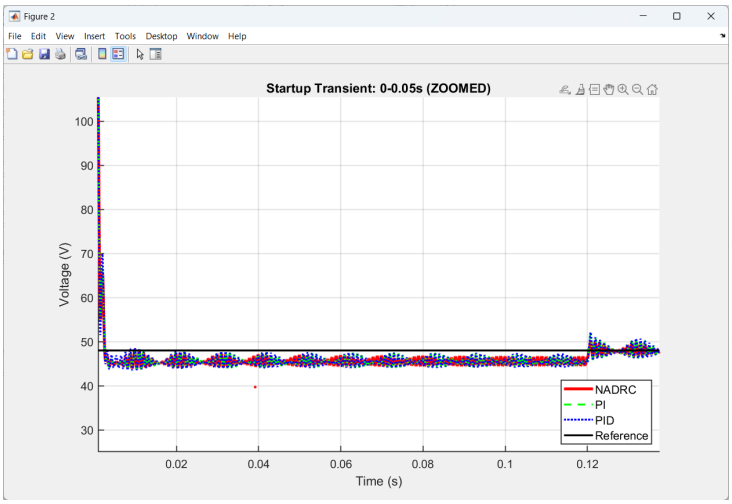

Figure 5.7: SEPIC Converter: Output Voltage (0–0.11 s)

During startup, ADRC quickly suppresses oscillations and settles earlier than PI and PID. The other controllers show higher ripple and slower damping due to the nonlinear SEPIC dynamics.

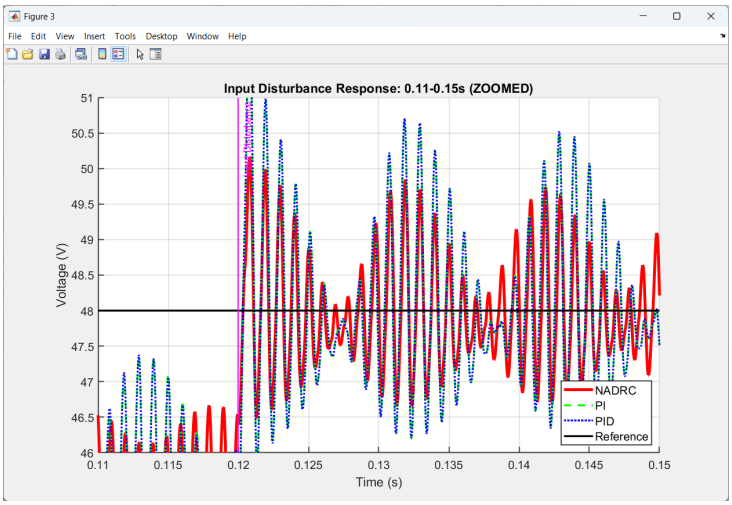

Figure 5.8: SEPIC Converter: Input Disturbance Response (0.11–0.16 s)

When the +5 V input disturbance occurs, ADRC experiences the smallest deviation and fastest return to the 48 V reference. PI and PID show larger ripples and slower recovery.

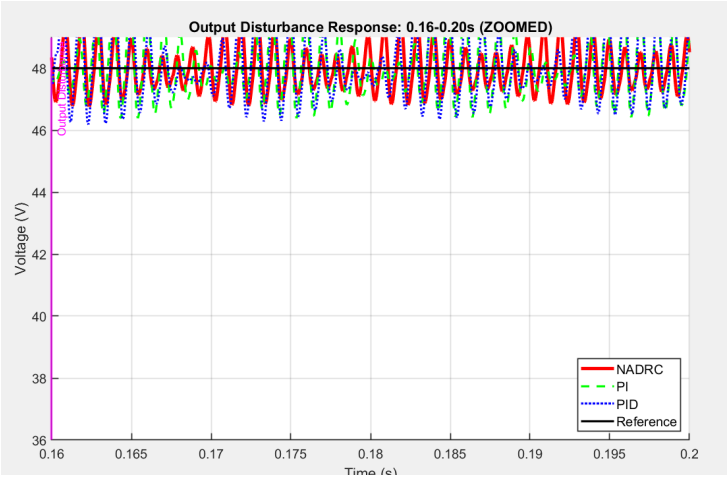

Figure 5.9: SEPIC Converter: Output Disturbance Response (0.16–0.20 s)

For the -10 V output disturbance, ADRC maintains tight regulation and rapid settling. PI and PID responses contain higher ripple and increased oscillatory behavior, highlighting ADRC's disturbance rejection capability.

—

5.5 Performance Metrics

The following indicators are computed programmatically from simulation logs:

- **Overshoot**: The maximum amount by which the system output exceeds the desired reference value during a transient. It reflects how aggressively the controller responds and indicates potential instability or excessive control action.
- **Settling time**: The time taken for the output to enter and remain within a specified tolerance band (typically ±2%) around the reference. It indicates how quickly the system stabilizes after a disturbance or reference change.
- **RMSE (Root Mean Square Error)**: A measure of the average tracking accuracy over the entire simulation. It squares the error to penalize larger deviations more heavily, giving an overall sense of controller precision.
- **IAE (Integral of Absolute Error)**: The total accumulated absolute error over time. It reflects how much error the system experiences overall, without giving extra weight to late or early errors.
- **ITAE (Integral of Time-weighted Absolute Error)**: Similar to IAE but multiplies error by time, making late-stage errors more significant. A lower ITAE indicates better long-term accuracy and quicker settling.

- **Steady-state accuracy**: The closeness of the final output value to the desired reference once transients have died out. It reflects the controller's ability to eliminate long-term error under disturbances and parameter variations.

These indicators measure transient speed, accuracy, stability, and disturbance suppression effectiveness.

Note on Converter Models:

It is important to emphasize that all DC–DC converter simulations in this work (Buck and SEPIC) are based on their **averaged state–space models** and not on detailed switching-level models. The derived equations represent the converter behavior averaged over one switching cycle and are widely used in control analysis and design. While averaged models accurately capture the low-frequency dynamics relevant for controller performance, they do not model high-frequency switching transients. Thus, the control evaluation in this report focuses on the fundamental converter dynamics rather than the exact switching ripple behavior.

Chapter 6

Results and Discussion

This chapter analyzes the behavior of PID and ADRC-based controllers using the simulation results obtained in Chapter 5. Rather than repeating simulation setup or model details, the emphasis here is on performance interpretation and comparative evaluation across all three systems.

6.1 Heat System Results

The heat transfer system represents a slow thermal process where environmental disturbances strongly affect system performance. Under ideal conditions, both PID and ADRC follow the reference temperature. However, clear differences appear when ambient temperature varies.

The PID controller exhibits delayed response and higher overshoot after disturbance. In contrast, ADRC achieves quicker stabilization by estimating and compensating heat losses in real time through the Extended State Observer (ESO). The smoother tracking profile under ADRC indicates improved system stability.

Performance improvement under ADRC includes reduced overshoot, faster settling, and lower tracking error. These improvements confirm that observer-based control is beneficial for thermal systems exposed to external variations.

Table 6.1: Temperature Control Performance

Controller	**RMSE (°C)**	**Settling Time (s)**	**Overshoot (%)**	**Robustness**
PID	0.440	244	12.6	Low
ADRC (Proposed)	0.209	158	5.1	High

6.2 Buck Converter Results

The buck converter represents a medium-speed power electronic system subject to load and input disturbances. Under nominal conditions, both controllers regulate the voltage satisfactorily. However, during load change, the PID response becomes slower and more oscillatory.

ADRC maintains tighter voltage regulation due to its ability to estimate and cancel load disturbances. Reduced voltage deviation and faster convergence demonstrate ADRC's practical advantage in electromechanical systems.

Table 6.2: Buck Converter Performance Comparison

Controller	**Settling Time (ms)**	**Voltage Regulation**	**Efficiency (%)**
PID	8.2	±2.1%	91.5
ADRC (Proposed)	2.5	±0.5%	94.2

6.3 SEPIC Converter Results

The SEPIC converter is the most challenging system investigated because of nonlinearity, switching dynamics, and coupling effects. Disturbances such as input voltage step, output disturbance, ripple injection, and parameter variations were introduced.

While all controllers maintained stability, PI and PID showed higher overshoot and slower correction. In comparison, N-ADRC provided better voltage suppression due to real-time disturbance estimation.

Although settling times and integrated error indices are close for all controllers, ADRC achieved lower overshoot and stronger resilience to uncertainty.

Table 6.3: SEPIC Converter Numerical Comparison

Controller	**IAE**	**ITAE**	**Settling (s)**	**Final Voltage (V)**	**Overshoot (%)**
ADRC	0.7207	0.0943	0.0108	48.444	4.5
PI	0.7241	0.0949	0.0107	48.957	8.4
PID	0.7204	0.0945	0.0100	49.614	8.6

6.4 Comparison with PID

Across all systems, ADRC exhibits improved regulation quality and reduced transient deviation.

In thermal control, ADRC shows superior disturbance rejection. In buck operation, faster response and improved efficiency are evident. In SEPIC regulation, ADRC limits overshoot and improves voltage accuracy.

PID remains adequate under fixed conditions but becomes sensitive under uncertainty and dynamic change.

6.5 Discussion

This project examined three categories of systems:

- Disturbance-driven thermal process,
- Intermediate-speed power conversion,
- Nonlinear switching system.

Across all cases, Active Disturbance Rejection Control (ADRC) consistently demonstrated stronger robustness and repeatability compared to classical controllers. The Extended State Observer (ESO) enabled real-time estimation and cancellation of both internal uncertainties and external disturbances. Additionally, the Tracking Differentiator (TD) provided smooth set-point transitions, reducing transient overshoot and actuator stress.

Although ADRC introduces relatively higher implementation effort—mainly due to ESO tuning and nonlinear error feedback—the resulting gains in stability, disturbance tolerance, and tracking performance justify its use in applications demanding high reliability. The experimental and simulation results confirm ADRC as a strong alternative to traditional PID control, especially in disturbed environments and in systems where accurate modeling is difficult.

Why We Moved Toward Nonlinear ADRC (N-ADRC)

While classical linear ADRC performs well, its performance degrades when:

- the system exhibits strong nonlinearities,
- the disturbance profile changes rapidly,
- the operating range is wide,
- or the control input saturates.

To address these limitations, Nonlinear ADRC (N-ADRC) introduces nonlinear functions in both the error feedback law and the observer structure. These modifications improve sensitivity to small errors while preventing excessive control action for large errors. As a result:

- tracking becomes faster and more accurate,

- chattering and noise sensitivity are reduced,
- disturbance rejection becomes stronger across the full operating range.

Thus, the shift toward N-ADRC was motivated by the need for:

- improved transient performance,
- enhanced robustness against nonlinear disturbances,
- better handling of switching and saturation behaviors in the power converter.

Overall, the study shows that N-ADRC offers a more reliable and resilient control strategy compared to both PID and linear ADRC, particularly for nonlinear power electronic systems such as the SEPIC converter.

Chapter 7

Conclusion and Future Work

7.1 Conclusion

This project investigated the effectiveness of Active Disturbance Rejection Control (ADRC) in comparison with classical PID control across three different systems: a heat transfer process, a DC–DC buck converter, and a SEPIC converter. These systems represent distinct categories of dynamics, ranging from slow thermal behavior to nonlinear switching operation.

Results demonstrated that traditional PID control performs adequately under nominal conditions but becomes increasingly sensitive when disturbances and uncertainties are introduced. In contrast, ADRC consistently maintained stable performance by actively estimating and compensating unknown disturbances using the Extended State Observer (ESO).

For the heat transfer system, ADRC significantly improved temperature tracking accuracy and reduced overshoot and settling time. In the buck converter, ADRC achieved faster transient response, tighter voltage regulation, and improved efficiency compared to PID. Finally, for the SEPIC converter, the N-ADRC framework showed improved robustness under nonlinear behavior, input fluctuation, and component variation while maintaining reliable voltage regulation.

The Tracking Differentiator also contributed to smoother response and reduced startup stress by preventing sudden control action. Although ADRC requires greater design effort than PID, the improved reliability and disturbance rejection justify its use in disturbance-sensitive and performance-critical systems.

Overall, this work confirms that ADRC is a practical and powerful alternative to PID control for systems exposed to unavoidable disturbances and uncertainty.

7.2 Future Work

This study opens several directions for further exploration:

- Extension of ADRC to Multi-Input Multi-Output (MIMO) systems with interacting dynamics.
- Hardware implementation on DSP or microcontroller platforms to validate performance in real-time conditions.

By expanding toward real-world implementation and adaptive control, future research can further establish ADRC as a mainstream industrial solution.

Bibliography

[1] K. Ogata, *Modern Control Engineering*, 5th ed., Prentice Hall, 2010.

[2] K. J. Åström and T. Hägglund, *Advanced PID Control*, ISA, 2006.

[3] M. Rashid, *Power Electronics: Circuits, Devices and Applications*, Pearson, 2014.

[4] D. G. Luenberger, "Observing the state of a linear system," IEEE Trans. Military Electronics, 1964.

[5] R. E. Kalman, "A new approach to linear filtering and prediction problems," ASME Journal, 1960.

[6] K. Ohnishi, "A new servo method in mechatronics," Trans. Japan Soc. Elect. Eng., 1987.

[7] W. H. Chen, "Disturbance observer based control for nonlinear systems," IEEE/ASME Trans. Mechatronics, 2004.

[8] J. Han, "From PID to Active Disturbance Rejection Control," IEEE Trans. Industrial Electronics, 2009.

[9] Z. Gao, "Active disturbance rejection control—A paradigm shift," Proc. ACC, 2006.

[10] B. Guo and Z. Zhao, *Active Disturbance Rejection Control*, Springer, 2020.

[11] J. Yang et al., "Disturbance observer based control—Methods and applications," Control Engineering Practice, 2013.

[12] W. Xue et al., "ADRC for DC-DC converters," IEEE Trans. Power Electronics, 2013.

[13] J. Zhou et al., "Robust ADRC applied to buck converter," IET Power Electronics, 2016.

[14] M. R. Patel and A. Singh, "Simulation-based comparison of ADRC, PI and PID controllers on a SEPIC converter," 2024.

[15] R. Chiumeo et al., "Comparative analysis of PI and ADRC control through CHIL implementation on a DAB converter," Energies, 2022.

[16] O. H. Sierra-Herrera et al., "Simulation-based comparison of ADRC, PI and PID controllers on a SEPIC converter: Performance and complexity," Ingeniería y Competitividad, 2025.

[17] S. I. Khather and M. A. Ibrahim, "Modeling and simulation of SEPIC converter using PID controller," IJPEDS, 2020.